AIAA'87

AIAA-87-2662
Acoustic Transmissibility of Advanced Turboprop Aircraft Windows

F.W. Grosveld, NASA Langley Research Center, Hampton, VA

AIAA 11th Aeroacoustics Conference

October 19-21, 1987/Palo Alto, California

ACOUSTIC TRANSMISSIBILITY OF ADVANCED TURBOPROP AIRCRAFT WINDOWS

Ferdinand W. Grosveld
The Bionetics Corporation
NASA Langley Research Center
Hampton, VA 23665-5225

Abstract

Advanced turboprop technology allows propeller aircraft to reach cruise speeds comparable to current jet aircraft yet with considerable fuel savings. Due to the higher blade loading and higher tip speed of these propellers, noise levels of up to 150 dB are expected on the outside of the fuselage in the propeller plane. In this study the transmissibility of triple pane windows, designed to provide 69 dB noise transmission loss at the blade propeller frequency of 164 Hz, was experimentally investigated using insertion loss and three-dimensional intensity techniques. A modal analysis on the outer window panes was conducted to determine pane modal frequencies. Coherence and phase relation of outer panes and window frame were established to obtain double/triple wall and lump mass resonance frequencies. Double/triple wall resonances were found to degrade the transmission loss of the two windows. It was shown that, at the blade passage frequency and the first two overtones, the combinations of window plus scratch shield provide less transmission loss than the average transmission loss of the treated fuselage. Strong disagreement was obtained between the experimental transmission loss of this investigation and the theoretical predictions from another study.

Introduction

Advanced technologies in the areas of aerodynamics, propulsion, structures, and production methods are incorporated in the design of the Advanced Turboprop (ATP) aircraft. Forward speed is designed to be comparable with jet aircraft, yet up to 30 percent in fuel savings can be realized. The propeller design typically consists of 8 to 12 highly loaded, swept blades in single or counter-rotating configuration and is expected to generate higher exterior noise levels than the propeller design on current aircraft. Analytical and experimental studies[1,2] have shown that acceptable cabin noise levels for these advanced turboprop aircraft can be achieved by using appropriate fuselage sidewall designs. For an efficient sidewall design, the window and supporting wall would need to have the same acoustic transmission characteristics at the critical turboprop frequencies.An analytical and parameter design study was performed in ref. 3 resulting in two triple pane window configurations that would provide 69 dB noise transmission loss at an estimated full-scale blade passage frequency of 164 Hz. This would reduce peak external surface sound pressure level of 150 dB to an acceptable 75 dBA inside the cabin. Acoustic transmissibility of aircraft type windows has been addressed in several publications,[4-7] but no experimental data are available for the triple pane window designs of ref. 3. The purpose of this paper is to report on a laboratory investigation of the transmissibility of the two window configurations as specified in ref. 3 and compare the experimental results with the transmission loss predictions made in that reference. The primary frequency range of interest covers the one-third octave bands 125 Hz - 630 Hz which include the blade passage frequency and three harmonics. The experimental transmission loss is obtained using insertion loss and three-dimensional intensity techniques.

Window Designs

The aluminum frames of the window designs measure 31.8 cm by 39.4 cm by 5.6 cm and contain three 25.4 cm by 33 cm window panes with a transparent area of 21.6 cm by 29.2 cm. A picture of one of the windows is shown in fig. 1. The heaviest of the two windows is designated Window I and has a total surface density of 51.7 kg/m^2. Two of the three panes are made of 0.94 cm thick glass and separated by an airspace of 0.79 cm. The third pane, made of acrylic for safety considerations, is 0.64 cm thick and is separated from one of the glass panes by a 2.54 cm airspace. When the window is installed, the acrylic pane faces the inside of the fuselage cabin. Window II, with a surface density of 44.9 kg/m^2, has the same configuration as Window I, except that the glass pane in the middle is replaced by a 0.64 cm thick pane while preserving the spacing with the other glass pane. The panes are supported by strips of elastomer kept in place with a contact cement. Silicon rubber is used to secure the windows in a 6.4 cm deep aluminum frame. A sketch of the Window I configuration is shown in fig. 2.

Window Resonance Frequencies

System resonance frequencies can adversely affect the transmission loss characteristics of the triple pane window. For window designs like the ones in the current investigation five types of resonances are expected to occur

1) Lump mass resonances. The bulk of the window, including the frame, is resonating. The boundary conditions, the way in which the window is supported, determine the stiffness and the damping of the system.

2) Single pane modal resonances. The vibrational response of the pane is decomposed in mode shapes with characteristic modal damping and modal frequencies.

3) Double and triple wall resonances. The fluid in between the panes acts as a spring and the vibration of two opposing panes are out of

Aerospace Research Engineer, Associate Fellow AIAA

4) Coincidence frequencies. The trace wavelength of a forcing acoustic wave matches the free flexural wavelength in the pane.

5) Cavity resonances. Half the acoustic wavelength matches the interpane spacing.

Simple calculations showed that the latter two types are well above the frequency range of interest. To determine single pane modal resonances, a modal analysis was performed by obtaining transfer functions between impulse excitation by a force-gauge-equipped hammer and the acceleration response of the pane at several locations on the pane surface. The windows, during these experiments, were supported by rubber strips underneath the aluminum frame.

It was assumed that at frequencies close to the natural frequencies of the pane, the inertance can be approximated to that of a single degree-of-freedom (SDOF) system plus a constant off-set term. For lightly damped structures the peak response will occur very close to its natural frequency. The circular nature of a modulus/phase polar plot (Nyquist plot) of the frequency response function of a SDOF system allows extraction of the modal parameters by curve fitting a circle through a few data points. These SDOF curve fits provide enough accuracy for well separated modes. The resulting modal frequencies and damping in the frequency range of interest are tabulated in Table I for the outer panes of Windows I and II.

The modal frequencies of the three different window panes were calculated for simply supported boundary conditions with[8]

$$f_{\ell,n} = \frac{\pi}{2}\left[\frac{Et^2}{12(1-\nu^2)m}\right]^{1/2}\left[\left(\frac{\ell}{a}\right)^2+\left(\frac{n}{b}\right)^2\right] \qquad (1)$$

where t is the thickness, m is the surface density and a and ℓ are the width and the length of the window panes (Table I). The Young's modulus E and Poisson's ratio ν for the acrylic pane were taken as $0.31 \cdot 10^{10}$ N/m^2 and 0.4, respectively. For the glass panes, these material properties were $6.2 \cdot 10^{10}$ N/m^2 and 0.24, respectively. Reasonable agreement is obtained between calculated and experimental values of the 1,2 and 2,1 modes of the acrylic pane and the fundamental mode of the outer glass pane. This suggests that the boundary conditions, where the panes are supported as shown in fig. 2, are closely approximated by simply supported. The inner glass pane was not accessible for analysis. The 1,1 mode and 1,3 mode of the acrylic pane could not be obtained as their response was obscured by other resonance behavior which will be discussed next.

To obtain lump mass and double/triple wall resonances, transfer functions in the form of Bode diagrams were obtained between normal acceleration responses of the two outer panes and the window frame. For that purpose accelerometers were attached to the centers of the acrylic pane and the glass pane and to one of the corners of the aluminum frame. Fig. 3 shows the relative magnitude of a transfer function between the response of an accelerometer in the center of the acrylic pane of Window I and the input of an impact hammer right next to it. This transfer function exhibits dominant responses at 196 Hz and 516 Hz. Similarly, dominant relative magnitudes were found at 183 Hz and 472 Hz for Window II. These resonances and their damping factors are tabulated in Table I. Also in this table is the range of calculated double wall frequencies for combinations of two panes with the third pane omitted. The response of these resonances was the cause of not being able to extract the modal parameters of the 1,1 and 1,3 modes of the acrylic pane. To further investigate if these resonances are of the double/triple wall type the coherence between the acceleration signals was measured to obtain a measure of their linear causality. Table II shows that at 196 Hz (Window I) the coherence between all combinations of the outer panes and the frame was exactly one. Similarly, very high coherence was found for these combinations at 516 Hz. The coherence at these frequencies was a local maximum in all cases. Examination of the phase relation between the acceleration of the outer panes showed that at 196 Hz (Window I) the acrylic pane and the outer glass pane move out of phase, typical for a double wall type behavior. At 516 Hz (Window I) the acrylic and the outer pane move in phase. At both frequencies the frame moves out of phase with the acrylic pane. To ensure that these resonances were not caused by a vibration of the entire window, since there is a high coherence between combinations of the outer pane and the frame, the rubber strips supporting the window were removed. The changed boundary conditions did not change any of the single pane nor double/triple wall frequencies. However, the change in support for the window did change the previously found resonance at 65 Hz and shifted it to 103 Hz. This suggests a lump mass resonance at that frequency. Table II shows high coherence between all combinations of outer panes and the frame. It also shows that the frame and glass move exactly in phase with a coherence of almost one. The acrylic pane, however, shows local minima in coherence with the glass pane and the frame and has no specific phase relation (0, -180 or 180 degrees) with either one. This can easily be explained by the fact that the calculated resonance frequency (126 Hz) of the acrylic pane is relatively close to the 103 Hz lump mass resonance. The acyrlic pane apparently is partially vibrating at its own resonance while the outer glass pane and the frame resonate as a lump mass.

Finally, it is interesting to compare the lump mass and double/triple wall behavior with a single pane modal response. The 2,1 mode of the acrylic pane of Window I (384 Hz) shows almost zero coherence with the glass pane, but very high coherence with the frame (Table II). The frame, with much lower resonance frequency, is more easily excited (lower transmissibility) than the outer glass pane which has a measured fundamental resonance frequency of 557 Hz (Window I). The acrylic pane and the frame move in phase while no specific phase relation is observed between the movement of the acrylic pane and the outer glass pane.

Window Transmission Loss

Predictions

A theoretical parameter study was performed in ref. 3 to establish specifications for acoustic window designs for advanced turboprop powered aircraft. The study was based on the approach taken in ref. 13. The transmission loss was calculated from the pressure ratio across the multi-layered configuration which can be expressed in terms of the pressure ratio across the individual layers. This pressure ratio can be calculated if both the characteristic and termination impedances of the layers are known. The parametric studies were performed for normal sound incidence conditions. Over 200 configurations for a multiple pane design were analysed and the designs of Window I and Window II were selected. The predicted transmission losses of these window designs with and without a scratch shield installed are graphically depicted in fig. 4. Indicated in this figure are the fundamental blade frequency (164 Hz) and the second (328 Hz) and third harmonic (492 Hz). The fourth harmonic (656 Hz), although not indicated in the figure, is within the frequency region of interest. These harmonics appear in the 160 Hz, 315 Hz, 500 Hz and 630 Hz one-third octave bands, respectively.

Insertion Loss

Test Facility.- Measurements were carried out in the NASA Langley Research Center Transmission Loss Apparatus.[9] The wall that separates the receiving and source rooms was modified through the addition of lead, concrete and other mass treatment to provide an estimated 57 dB transmission loss at 160 Hz, which is the equivalent of a 50 cm thick concrete wall. To increase transmission loss at higher frequencies one-foot-thick foam blocks were inserted filling the space between the walls of receiving and source rooms. The background noise in the receiving room was measured to be less than 35 dB in each one-third octave band in the frequency range of 125 Hz - 1000 Hz. In the opening between the two rooms a 8.9 cm thick particle board panel (1.22 m by 1.52 m) was installed to support either one of the window designs. The particle board insert was of much higher surface density (82.9 kg/m^2) than the window designs exhibiting an inherently higher transmission loss. Due to the size of the window designs, the lay-out and size of the source and receiving rooms, the frequency range of interest and the expected high transmission loss of the windows it was not possible to test these windows according to the standard of the American Society of Testing Materials (ASTM).[10] To minimize any effect of flanking paths through the particle board support panel the transmission loss was determined by insertion loss measurements and the highest incident sound pressure levels were concentrated at the windows surface. For that purpose a pneumatic horn was used with a sound pressure level distribution on the source side as depicted in fig. 5. The use of the horn provides a way to simulate close to normal sound incidence on the windows since the transmission loss predictions in ref. 3 were made for those conditions. The exponential horn is 2.13 m long with a mouth diameter of 0.61 m and a flare constant of 2.60 m^{-1}. The horn is driven by low-pressure air (40 psi) in combination with a white noise generator. Its cut-off frequency is calculated to be at 71 Hz. The test set-up is depicted in fig. 6. The mouth of the horn is located 0.5 cm from the window surface.

Insertion Loss Measurements.- Insertion loss of the window is defined as the difference between the sound pressure level in the receiving room due to a noise source in the source room without and with the window installed. The sound pressure level in the receiving room was measured by a opposite from the window. At that location all room modes will have their highest sound pressure amplitude. The sound pressure level at the receiver microphone, measured without the panel installed, includes any flanking through the particle board structure, room modes and absorbtion in the receiver room and directivity of the noise source. When the panel is installed the sound pressure level at the receiver microphone includes all these effects plus the effect of sound blocked by the window. The insertion loss is thus a measure of how much sound is transmitted through the window. A measure of the sound incident on the window was represented by the sound pressure level at the location of the window, without the window installed. The ratio of this "incidence" sound pressure level and the insertion loss is then an approximation of the ratio of incident and transmitted power, which is the definition of transmission loss. To verify the validity of these assumptions, a thin acrylic panel with a surface density of 3.78 kg/m^2 was installed onto the support panel and separated by a thin layer of silicone rubber to simulate simply supported boundary conditions. Transmission loss obtained from the measured insertion loss and the "incident" pressure of this panel is compared with calculated transmission loss for normal sound incidence. In the higher frequency region, where its behavior is governed by its mass m this transmission loss is represented by[10]

$$R \approx 10 \log \left[1 + \left(\frac{\omega m}{2\rho c}\right)^2\right] \qquad (2)$$

As shown in fig. 7, above the 200 Hz one-third octave band the measured transmission loss falls in between the calculated transmission loss for normal and field incidence of the incoming sound. For values over 12 dB, the normal incidence mass law is 5 dB higher than the field incidence mass law. This suggests that the transmission loss, approximated by measured insertion loss and "incident" pressure is comparable with the expected theoretical transmission loss. Using this procedure the transmission loss of the two window designs was determined and compared with their respective normal incident mass laws in fig. 7. At the one-third octave band center frequencies of 200 Hz and 500 Hz the transmission loss is considerably lower than expected from mass law behavior. As discussed in the previous section double/triple wall resonances degrade the transmission loss properties of the two windows at 196 Hz and 516 Hz. Other resonances occuring in the frequency range of interest do not strongly affect the transmission loss. As shown in Table 3 for the blade passage frequency and three overtones, these measured transmission loss values do not compare very well with predicted values from ref. 3.

Intensity

Test Facility and Equipment.- For the intensity measurements each of the windows was installed in a 1.22 m by 1.52 m fuselage sidewall panel. A mounting was designed and installed in the fuselage panel to accommodate each of the windows. The sidewall panel consists of a 0.114 cm thick aluminum skin reinforced by four 15.2 cm high frames with a spacing of 48.3 cm and eight 3.42 cm high stringers with a spacing of 15.2 cm. These stiffeners divide the fuselage panel into twenty-one equal bay areas. The fuselage panel was tested with and without a trim treatment installed. The treatment consists of a 0.93 cm thick visco-elastic layer attached to the skin and a 7.62 cm thick layer of fiberglass supported by a trim panel, separated by an air gap of 6.65 cm (fig. 8). The visco-elastic layer has a surface mass of 13.1 kg/m^2 and consists of a 0.29 cm thick loaded urethane elastomer bonded to 0.64 cm thick rubber. The trim panel is a combination of a 0.64 cm thick plexiglass panel adhered to a high strength-to-weight sandwich panel with laminated fiberglass facings and a core of blended plastic resins. In this configuration the treatment behind the window has been removed and replaced by a transparent 0.25 cm thick acrylic scratch shield attached to the trim panel leaving a spacing of 9.47 cm. The trim panel is decoupled from the window and sidewall to prevent structural flanking paths.

The intensity measurements were accomplished with a specially constructed four-microphone probe to obtain the intensity vector in three-dimensional space. The distance between the microphone centers was 50 cm, which was choosen to minimize errors that are due to residual phase and cross-channel phase differences in the frequency range of interest. The probe and its orientation with respect to the panel is depicted in fig. 9, where the positive x-axis is perpendicular to the back of the fuselage panel. The positive y-axis is pointing up while the z-axis is in horizontal direction and both the y-axis and z-axis are in the plane of the fuselage skin panel.

Intensity Measurements.- The sound intensity is a vector quantity which describes the amount and direction of net flow of acoustic energy at a given position. In a medium without mean flow, the intensity vector equals the time averaged product of the instantaneous pressure and the corresponding instantaneous particle velocity at the same position

$$\vec{I} = \overline{p(t) \cdot \vec{u}(t)} \qquad (3)$$

If the separation distance, Δr, is small compared with the wavelength, it can be shown[11] that the intensity vector component in the direction r can be calculated from

$$I_r = -\frac{1}{2\rho\Delta r} \overline{(p_A + p_B) \int (p_B - p_A)\, dt} \qquad (4)$$

needing only sound pressure level measurements from two microphones. This quantity I_r is referenced to an intensity of 1 pW/m^2. The measured intensity is corrected by a phase compensation function for the cross-channel phase difference that is observed in the system when the same signal is input into both channels of a pair. Computation of this phase compensation function is based on the principle that two identical signals should produce intensity functions with zero relative phase difference. For this purpose the four microphones of the intensity probe were mounted into pre-drilled holes in the pneumatic horn at equal distance from the source and as close together as possible without touching. Phase compensation functions for each channel pair were calculated from the imaginary and real part of the cross spectrum

$$\Delta\phi = \arctan \frac{\mathrm{Im}\, G_{AB}}{\mathrm{Re}\, G_{AB}} \qquad (5)$$

No changes were made in the system after this calibration procedure. The accuracy of the computed intensity is affected by a residual phase error at 0 Hz, while low and high frequency limitations are related to the 50 cm inter-microphone-spacing of the probe. In the frequency range of interest the estimated error is less than 1 dB. To aid in data acquisition, data processing and data management a Computer Aided Test (CAT) system was used. Intensity measurements were conducted on both sides of the fuselage panel at the center of each of the 21 bay areas confined by bordering stiffeners. At the window location an additional four measurements were taken near the corners of the window to provide more accuracy and detail in that area. On the source side of the fuselage panel measurements were conducted 2.54 cm from the skin surface. At the receiving side measurements took place in a plane at 0.5 cm from the back pane of the window and, when the trim was installed, in a plane 0.5 cm away from the transparent acrylic scratch panel. Intensity vectors at some measurement locations on the receiving side of the fuselage panel, with Window I installed, are graphically shown in fig. 10.

The Reactivity Index[12] is a measurement of the normalized random error in the measurements and is defined as the difference in intensity level L_I and sound pressure level L_p. It is related to the wave number k, the actual phase ϕ and the microphone spacing Δr by

$$L_K = L_I - L_P = -10 \log \frac{k\Delta r}{\phi} \qquad (6)$$

The Reactivity Index has been measured at the 25 measuring locations and is distributed over the fuselage panel as depicted in fig. 11. The data within the outer measurement locations is interpolated and no data is available outside this area. The box around the data in fig. 11 represents the outer dimensions of the fuselage panel. Highest Reactivity Index is a little over -7 dB. This means that the normalized random error in each one-third octave band between 160 Hz and 1250 Hz (68 percent confidence interval) is less than 1 dB for a phase mismatch of 0.3 degrees and a 50 mm microphone spacing.[11]

To validate the three-dimensional intensity vector method the experimental transmission loss of a thin acrylic panel with a surface density of 3.78 kg/m^2 is again compared with its field incident theoretical mass law in fig. 12. Except

for the 160 Hz and 250 Hz one-third octave bands good agreement was obtained in the frequency range of interest. It has to be noted that these experimental values are low (up to 5 dB lower) if they would be compared with the theoretical normal mass law. Also shown in fig. 10 is the experimental transmission loss for Windows I and II using the intensity vector method. Preference was given to the three-dimensional intensity method, rather than the normal component of the intensity, because of the directionality of the source and the complexity of the window designs and the treated sidewall. In a thin homogeneous material the impedance change does not substantially affect the directivity of the sound. The incident intensity vector and the transmitted vector have the same direction and their ratio is the same as the ratio of their normal components. For the triple pane window the angle of the transmitted vector is different due to impedance changes through the triple pane window and the treated sidewall. Hence, the three-dimensional intensity vector is more realistic. In addition, the measured transmitted sound is not only coming from one point on the structure, but rather from several different sources on the panel. The inclusion of more sources smoothes out the transmission loss curves. A comparison between the three-dimensional vector intensity and its normal component is shown in fig. 13 for Window I. The normal component intensity transmission loss is showing again the effects of double/triple wall resonances in the 200 Hz and 500 Hz one-third octave bands measuring only contributions perpendicular to the window. As other sources contribute (reflections off the inside of the window frame, etc.) the relative effect of window resonances is reduced for the three-dimensional intensity transmission loss.

In fig. 14 the transmission loss obtained with the vector intensity method is compared with the transmission loss obtained with the insertion loss method. Reasonable agreement is obtained (within 4 dB) for the frequency region of interest (125 Hz - 630 Hz). After installation of the trim the transmission loss was measured for the window designs I and II with the trim scratch shield in place on the trim panel (fig. 15). This data is compared with the average transmission loss of the treated sidewall. Table IV shows that the window plus the scratch shield exhibits up to 18-19 dB more transmission loss at the higher frequencies (1000 Hz). This increase is not only due to the added transmission loss but also due to absorption by the fiberglass in the cavity between the trim panel and the fuselage skin. At the blade passage frequency and two overtones the transmission loss of Windows I and II plus scratch shields are less than the average of the treated sidewall. In figs. 16 and 17 the transmission loss of the fuselage panel is depicted at the blade passage frequency and three overtones with respectively Window I and Window II installed. It was concluded that the windows, compared to the treated fuselage panel cause an acoustic leak. Finally, the measured transmission loss for Windows I and II, using the vector intensity method, is compared with the predicted data from ref. 3 in figs. 18 and 19. At the blade passage frequency (164 Hz) measured data are some 50 dB lower than predicted. Comparison of the data for the window with the trim panel (scratch shield) installed is of similar disagreement.

Conclusions

Experimental transmission loss was obtained for the window designs for ref. 3, with and without a scratch shield, using vector intensity and insertion loss techniques. When compared, the two experimental methods showed reasonable agreement. Both methods agreed favorably with theoretical predictions for a thin acrylic panel, that is believed to behave according to mass law in the frequency region of interest. It was shown that the window designs plus the scratch shields provide less transmission loss than the average transmission loss of the treated fuselage at the blade passage frequency and the first two overtones. Double/triple wall resonances were shown to degrade the transmisison loss characteristics of the two windows in the 200 Hz and 500 Hz one-third octave bands. With the treatment and scratch shield installed the degradation in transmission loss at these frequencies was partially relieved. Strong disagreement was obtained between experimental transmission loss of the two window designs, with and without scratch shield and fuselage treatment, when compared with theoretical predictions made in ref. 3.

Acknowledgments

This work was performed under NASA Contract NAS1-16978, Dr. C. A. Powell, Technical Monitor.

References

[1] Revell, J. D.; Balena, F. J.; and Koval, L. R.: Analytical Study of Interior Noise Control by Fuselage Design Techniques on High-Speed Propeller Driven Aircraft. NASA CR 159222, July 1978.

[2] Prydz, R. A.; Revell, J. D.; Hayward, J. L.; and Balena, F. J.: Evaluation of Advanced Fuselage Design Concepts for Interior Noise Control on High-Speed Propeller-Driven Aircraft. NASA CR 165960, September 1982.

[3] Prydz, R. A.; and Balena, F. J.: Window Acoustic Study for Advanced Turboprop Aircraft. NASA CR 16441, August 1984.

[4] Grosveld, F.; Navaneethan, R.; and Roskam, J.: Noise Reduction Characteristics of General Aviation Type Dual Pane Windows. AIAA Paper 80-1874, August 1980.

[5] Vaicaitis, R.: Study of Noise Transmission through Double Wall Aircraft Windows. NASA CR 172182, October 1983.

[6] Mixson, J. S.; O'Neal, R. L.; and Grosveld, F. W.: Investigation of Fuselage Acoustic Treatment for a Twin-Engine Turboprop Aircraft in Flight and Laboratory Tests. NASA TM 85722, January 1984.

[7]Grosveld, F. W.: Field-Incidence Noise Transmission Loss of General Aviation Aircraft Double-Wall Configurations. Journal of Aircraft, vol. 22, no. 2, February 1985, pp. 117-123.

[8]Leissa, A. W.: Vibration of Plates. NASA SP 160, 1969.

[9]Grosveld, F. W.: Characteristics of the Transmission Loss Apparatus at NASA Langley Research Center. NASA CR 172153, May 1983.

[10]"ASTM Standard Method for Laboratory Measurement of Airborne Sound Transmission Loss of Building Partitions." American Society for Testing Materials, Designation E90-81, Annual Book of ASTM Standards, Part 18, 1982.

[11]Gade, S.: Sound Intensity (Part I. Theory). Technical Review, Bruel & Kjaer Instruments, Denmark, No. 3, 1982.

[12]Roland, J.: What are the Limitations of Intensity Technique in a Semi-Diffuse Field. Inter Noise Proceedings, 1982, pp. 715-718.

[13]Cockburn, J. A.; and Jolly, A. C.: Structural-Acoustic Response, Noise Transmission Losses and Interior Noise Levels of an Aircraft Fuselage Excited by Random Pressure Fields. USF, AFFDL-TR-68-2, Wright Patterson AFB, Ohio, August 1968.

TABLE I. CALCULATED AND MEASURED WINDOW RESONANCE FREQUENCIES

				Calculated	Experimental			
				(Simply Supported)	Window I		Window II	
Resonance	System	Thickness [cm]	Mode	Frequency [Hz]	Frequency [Hz]	Damping Factor	Frequency [Hz]	Damping Factor
Single Pane	acrylic	0.64	1,1	126	---	---	---	---
			1,2	266	283	0.0243	261	0.0154
			2,1	363	384	0.0149	379	0.0129
			1,3	500	---	---	---	---
	glass	0.94	1,1	558	557	0.0275	585	0.0154
		0.64	1,1	380				
Double/ triple wall	acrylic/ glass/ glass			128-226*	196	0.0252	183	0.0238
					516	0.0160	472	0.0309
Lump mass	glass/frame				65 (103)	0.0604	69	0.1129

* Range of frequencies for double wall resonances

TABLE II. COHERENCE AND PHASE RELATION BETWEEN RESONANCE ACCELERATION OUTPUT FROM THE OUTER PANES AND THE FRAME OF WINDOW I.

	Coherence				Phase Difference (Deg)			
	Frequency (Hz)				Frequency (Hz)			
	103	196	384	516	103	196	384	516
Acrylic - Glass	0.87 (-)	1.00 (+)	0.03 (-)	0.98 (+)	~	-180	~	0
Frame - Glass	0.98 (+)	1.00 (+)	0.03 (-)	0.98 (+)	0	0	~	-180
Frame - Acrylic	0.80 (-)	1.00 (+)	0.97 (+)	0.95 (+)	~	180	0	180

(+) denotes maximum
(-) denotes minimum
~ other than 0, -180 or 180 degrees

TABLE III. COMPARISON OF TRANSMISSION LOSS DATA (dB) AT THE ATP BLADE PASSAGE FREQUENCY AND ITS FIRST THREE OVERTONES

Structure		One-Third Octave Band Center Frequency (Hz)			
		160	315	500	630
Window I	Measured	28.2	38.7	35.0	43.7
	Predicted (ref. 3)	83	80	79	68
Window II	Measured	26.3	39.6	33.9	38.4
	Predicted (ref. 3)	73	71	63	67

TABLE IV. COMPARISON OF TRANSMISSION LOSS DATA (dB) AT BLADE PASSAGE FREQUENCY AND THREE OVERTONES

Structure		One-Third Octave Band Center Frequency (Hz)			
		160	315	500	630
	Treated Panel (averaged)	34.2	51.8	60.8	58.3
	Window I	26.7	34.2	39.6	43.4
	Window II	23.8	32.9	36.2	43.6
With Scratch Shield	Window I	31.6	49.8	57.2	61.9
	Window II	28.7	48.4	53.8	62.1

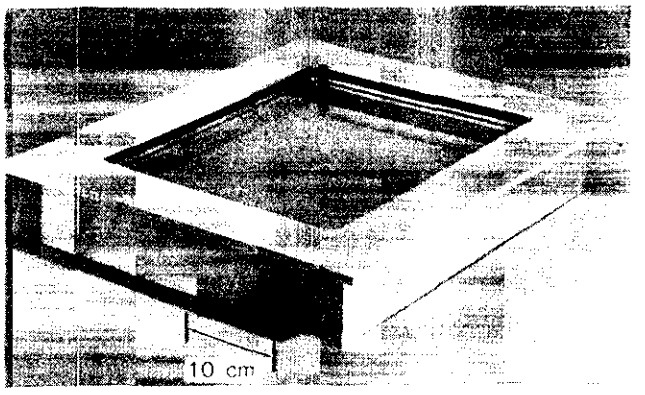

Fig. 1. Window design for the Advanced Turboprop aircraft.

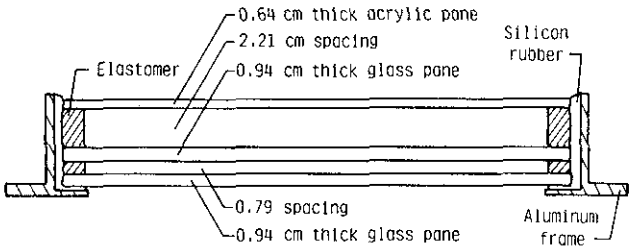

Fig. 2. Lengthwise cross-section of Window I.

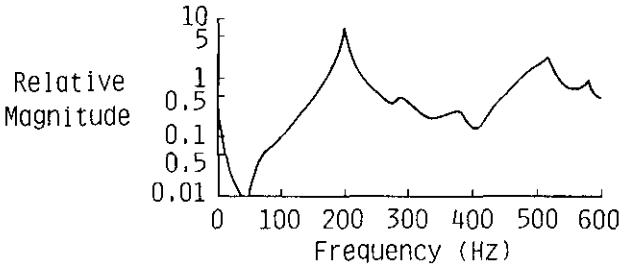

Fig. 3. Relative magnitude of transfer function between hammer impulse excitation and accelerometer response in center of Window I acrylic outer pane.

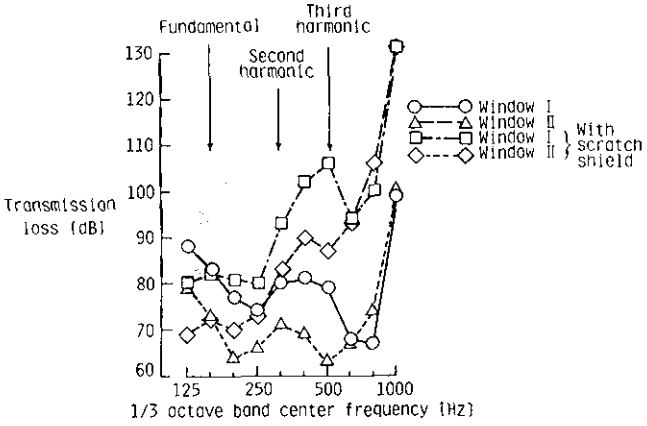

Fig. 4. Transmission loss predicted for triple-pane window designs (ref. 1)

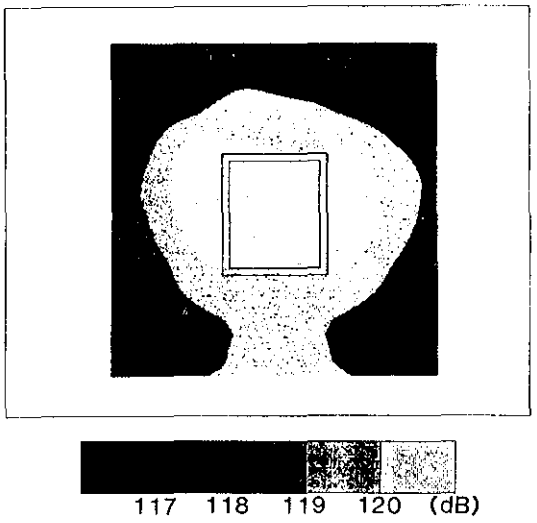

Fig. 5. Sound pressure level distribution on source side of fuselage panel.

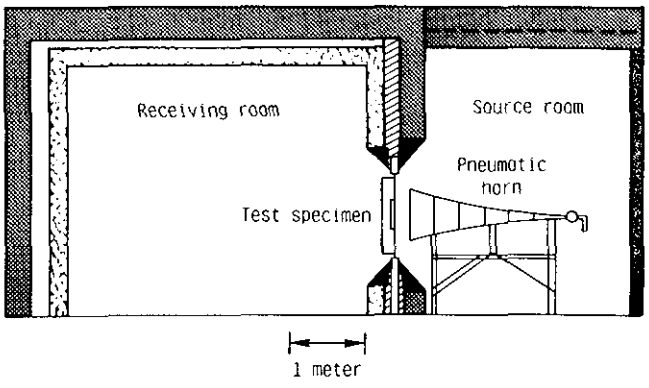

Fig. 6. Test configuration in the NASA Langley Research Center Transmission Loss Apparatus.

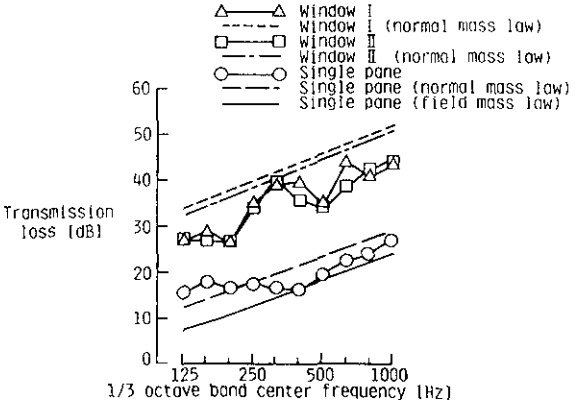

Fig. 7. Measured and predicted transmission loss for the two window designs and a single acrylic pane.

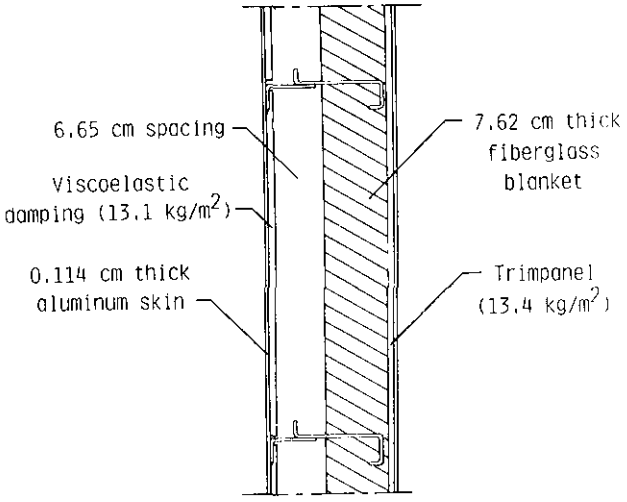

Fig. 8. Cross-section of fuselage sidewall construction with acoustic treatment installed.

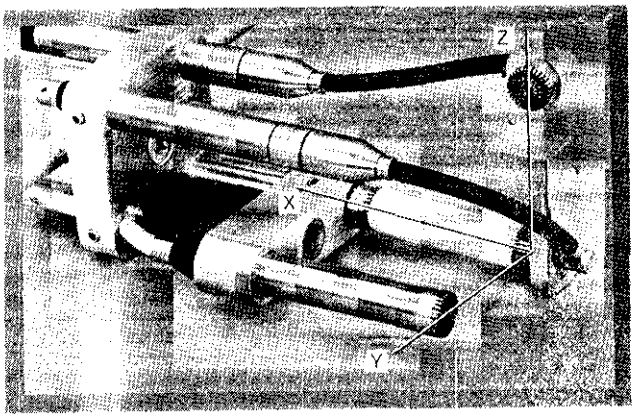

Fig. 9. Four microphone intensity probe with related Cartesian co-ordinate system.

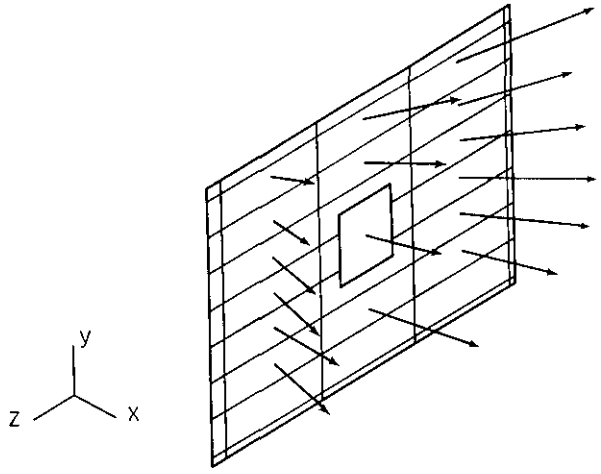

Fig. 10. Intensity vectors at some measurement locations on the back of the horn-excited bare fuselage panel. (Window I installed)

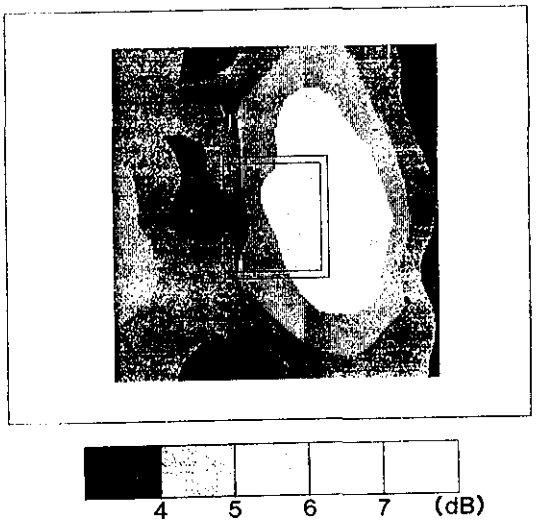

Fig. 11. Reactivity index distribution for bare fuselage panel.

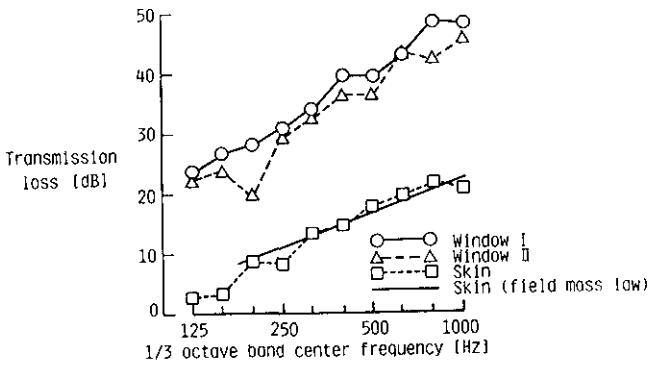

Fig. 12. Measured transmission loss for the two window designs and the fuselage skin using three-dimensional intensity vector method.

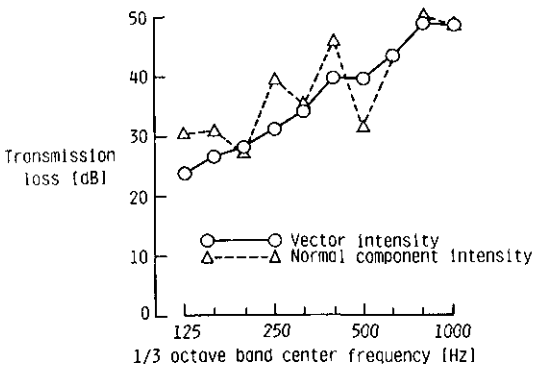

Fig. 13. Transmission loss of Window I using three-dimensional intensity vectors or their components normal to the panel.

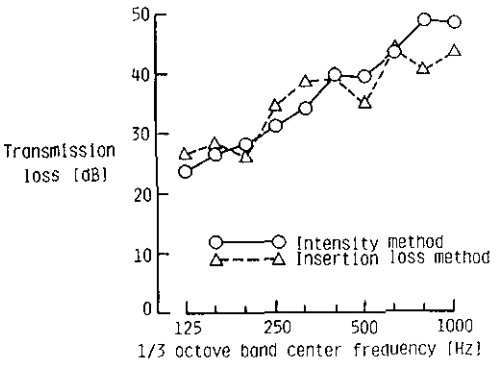

Fig. 14. Transmission loss of Window I using the insertion loss or intensity method.

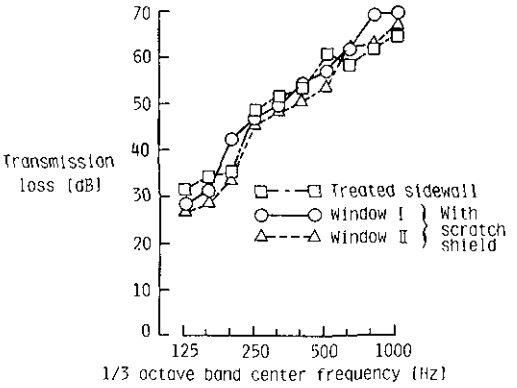

Fig. 15. Transmission loss (Intensity method) of the treated sidewall and the window designs with a scratch shield installed.

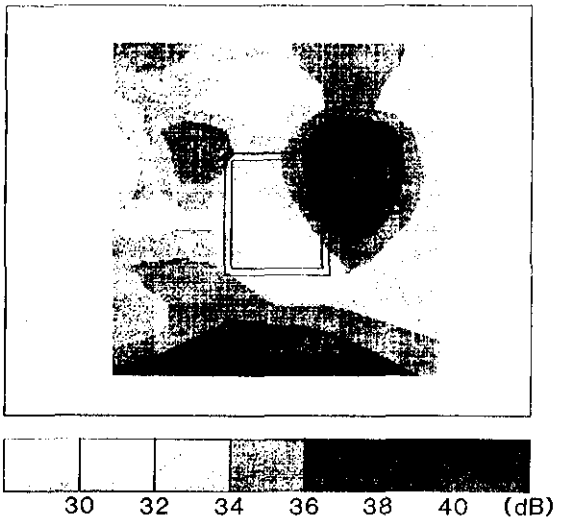

Blade passage frequency (164 Hz)

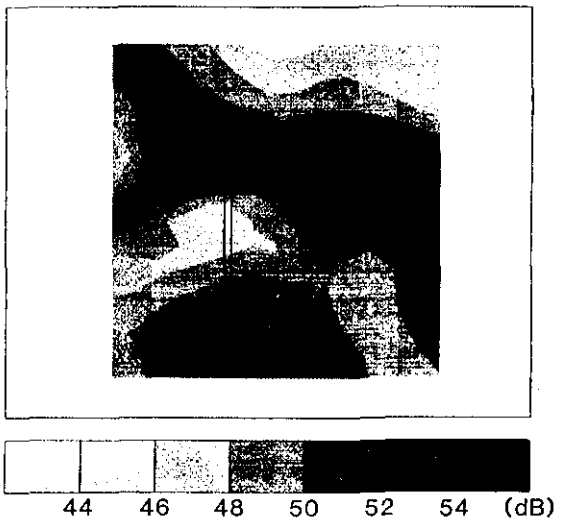

Second harmonic (328 Hz)

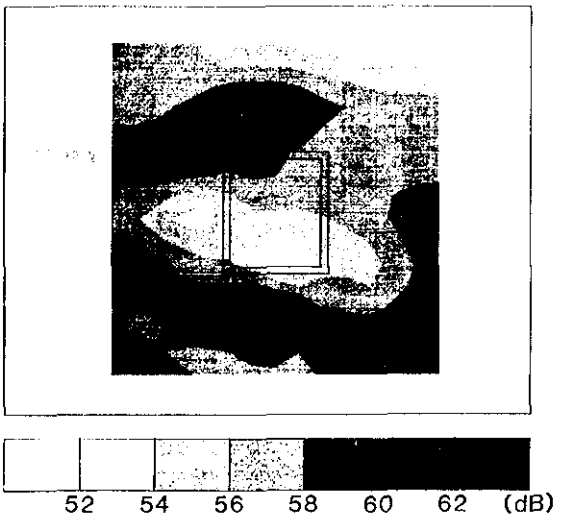

Third harmonic (492 Hz)

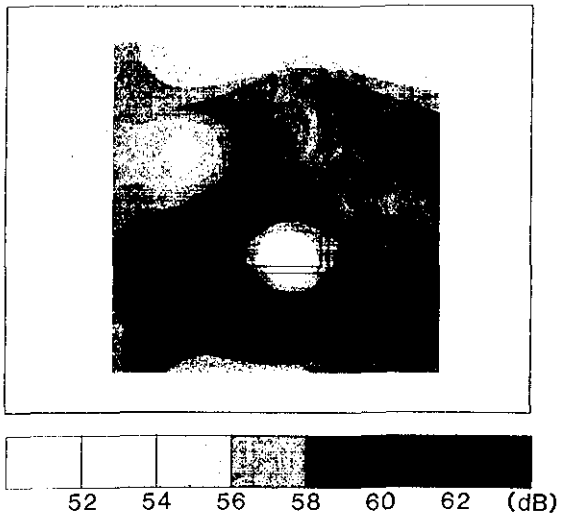

Fourth harmonic (656 Hz)

Fig. 16. Transmission loss distribution on treated fuselage panel with Window I installed.

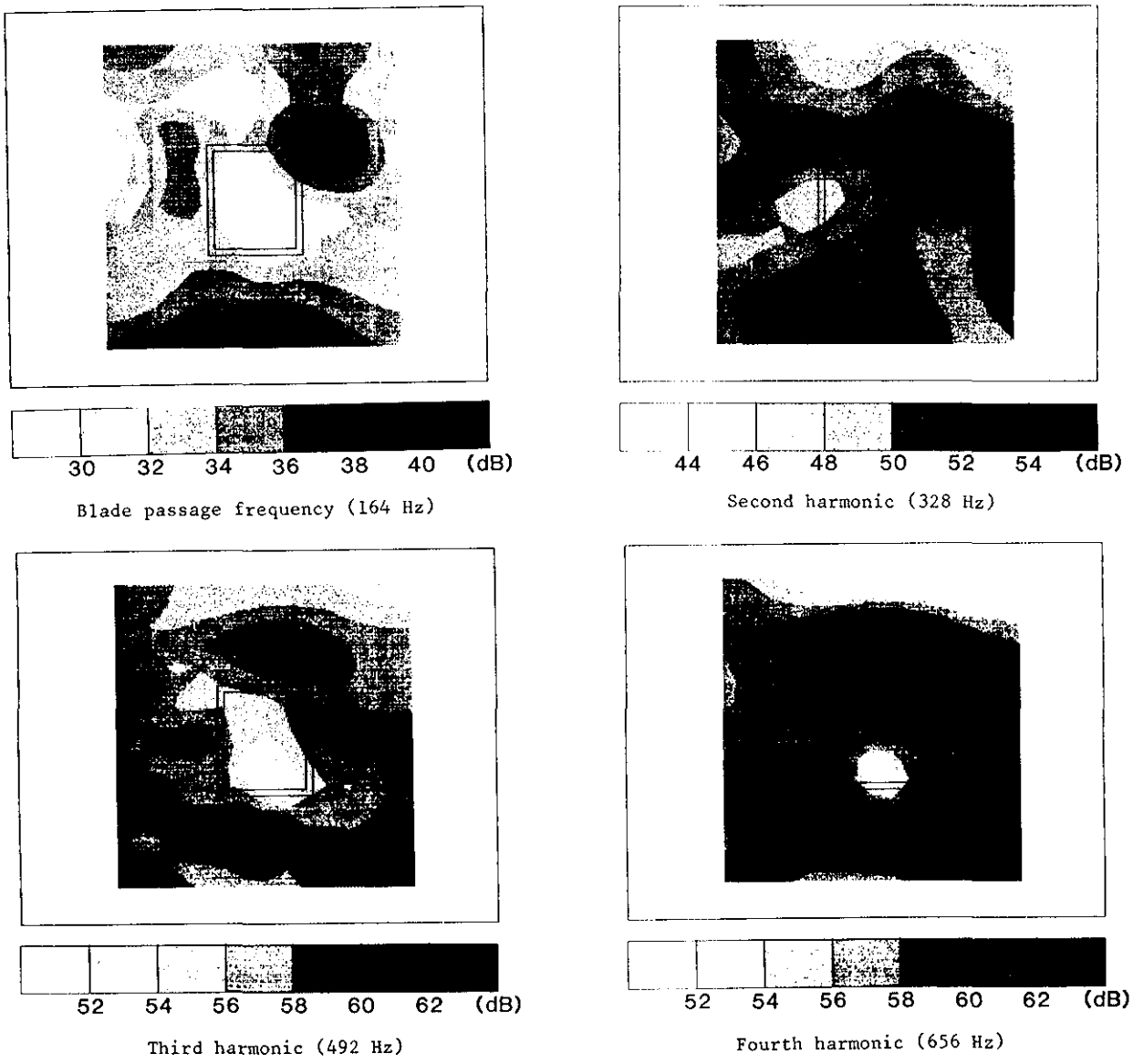

Fig. 17. Transmission loss distribution on treated fuselage panel with Window II installed.

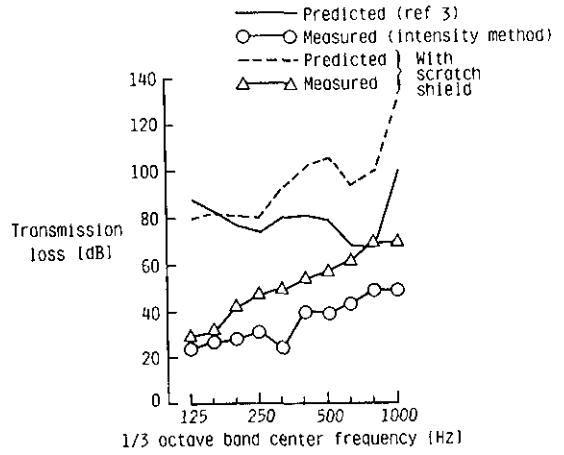

Fig. 18. Predicted (ref. 1) and measured transmission loss (Intensity method) of Window I with and without a scratch shield installed.

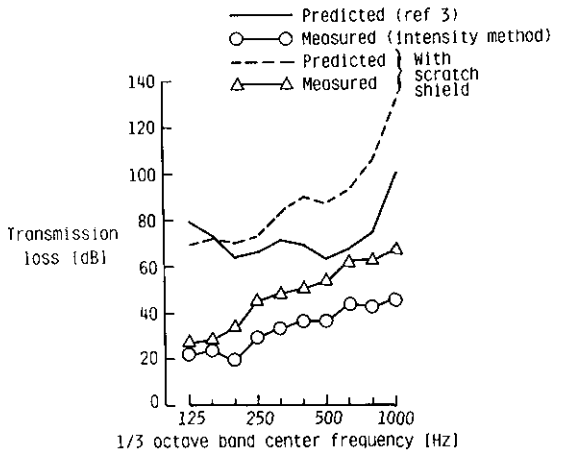

Fig. 19. Predicted (ref. 1) and measured transmission loss (Intensity method) of Window II with and without a scratch shield installed.